Surface Measurement Systems
World Leader in Sorption Science

iGC SEA & DVS Case Study 608

Characterizing Disorder in Pharmaceutical Materials by Vapor Sorption Techniques

Daniel Burnett, , Majid Naderi, Manaswini Acharya and Armando R. Garcia,
Surface Measurement Systems Ltd.

The thermodynamic stability of pharmaceutical materials affects all levels of formulation, process development and storage. Thermodynamic instability can range from highly ordered crystals with different polymorphs or solvates to completely amorphous materials. Vapor sorption techniques like Dynamic Vapor Sorption and Inverse Gas Chromatography are powerful tools in the identification and characterization of these materials.

Introduction

The majority of pharmaceutical materials can exist in a preferred crystalline state, characterized by an ordered lattice structure. However, there may be several different crystalline forms of the same material including polymorphs and/or solvated crystal forms. There will typically be one thermodynamically preferred crystal structure with the lowest energy. All other forms are considered metastable and will eventually relax to the more stable form. However, the timescales of these transitions may be long enough at typical storage and processing conditions for the metastable forms to be used for pharmaceutical development. Also, during the processing of pharmaceutical solids (e.g. crystallization, milling, spray drying, tablet compaction, wet granulation, and lyophilization), various degrees of disorder in the form of crystal defects and/or amorphous regions may be generated. In extreme cases, the material may be completely amorphous where there is no longer any long-range structural order. Amorphous materials in pharmaceutical formulations yield complex and challenging problems concerning the performance, processing, and storage of these products [1]. The presence of amorphous materials can be wanted or unwanted, depending on the desired or undesired unique properties of the amorphous state. Even relatively low levels of amorphous material (<10%), may have a detrimental impact on the stability and manufacturability of the formulated drug product. Disordered materials are inherently metastable and provided with thermal or mechanical energy will tend to revert to a more thermodynamically stable, crystalline form. For these reasons, investigating the level of disorder or thermodynamic state of pharmaceutical materials is critical in their formulation, storage and processing.

This overview paper highlights how vapor sorption techniques can be used to study pharmaceutical solids ranging from the lowest-energy crystalline state, to higher energy polymorphs and solvates, to defect sites, to completely amorphous materials. Dynamic Vapor Sorption (DVS) and Inverse Gas Chromatography (IGC SEA) are well-established techniques used for the determination of surface and bulk properties of powders, fibers, and films. The aim of this paper is to focus on the applications of

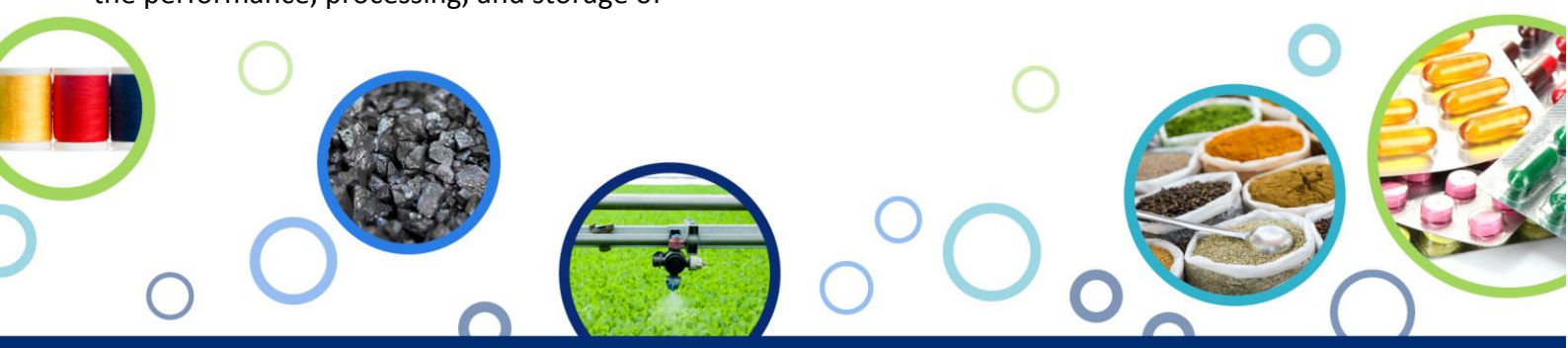

these techniques as they relate to thermodynamic stability in pharmaceutical materials.

Method

Gravimetric vapor sorption methods have been widely used to study the interaction of water with pharmaceutical materials [2,3]. DVS is a well-established method for the determination of vapor sorption isotherms. The DVS measures the sample mass change as the vapor environment surrounding the sample is varied in a controlled manner. An increase in mass is typically associated with vapor sorption, while a decrease is due to vapor desorption. The vapor concentration around the sample is controlled by mixing saturated and dry carrier gas streams using electronic mass flow controllers.

The basic principles of IGC SEA are very simple, being the inverse of a conventional GC experiment. However, unlike analytical GC, IGC SEA is a physico-chemical characterization technique, not an analytical technique. To run an IGC SEA experiment, a column is first packed or coated with a solid material of interest, typically a powder, fiber, film, or coating. A pulse or constant concentration of a known vapor or gas probe is then injected down the column at a fixed carrier gas flow rate and the retention behavior of the pulse or concentration front is measured by a detector. A series of IGC SEA measurements with different gas or vapor phase probe molecules thus allows access to a wide range of physicochemical properties of the solid sample. The fundamental parameter from which most physicochemical properties are derived is known as the retention volume, V_N, a measure of how strongly a given vapor probe molecule interacts with the solid sample. From this retention volume, the surface energy, solubility parameter and other physical properties of a pharmaceutical material are derived. Several in-depth reviews of the theory and application of IGC SEA can be found in the open literature [4,5,6,7].

Crystalline Materials

The most thermodynamically stable form of a pharmaceutical solid will be the lowest energy crystalline state. This material will have the lowest free energy value compared to the less stable forms. Also, the surface free energy will be independent of particle size alone. This is illustrated in Figure 1 for crystalline α-lactose monohydrate. Crystals were sieved to different particle size fractions yielded identical dispersive surface energy values. Therefore, any changes in surface energy will be due to a change in surface chemistry or orientation of surface groups, not particle size alone.

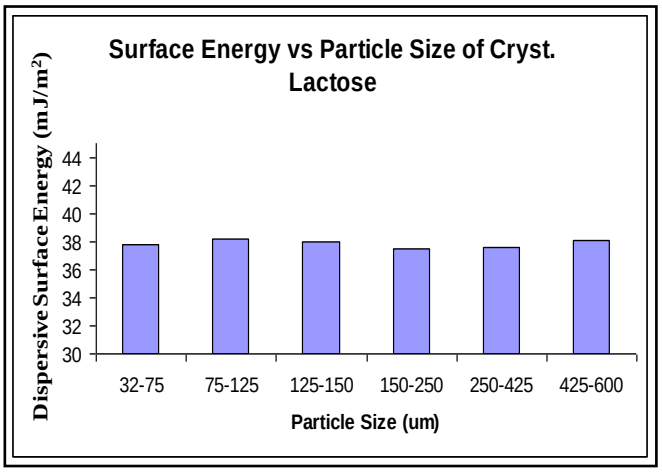

Figure 1. Dispersive surface energy values for α-lactose monohydrate crystals at different particle size fractions.

Polymorphs

As mentioned previously most materials will have a thermodynamically preferred crystalline configuration. However many pharmaceutical solids can exhibit polymorphism, which is the ability of a substance to exist as two or more crystalline phases that have different arrangements of the crystal lattice [8]. Each polymorph will be associated with a different energy, with one configuration being more stable. The less stable forms will ultimately relax to the more stable form, but these transitions can have quite high activation barriers at typical storage and processing conditions leading to metastable polymorphs [9]. Different polymorphs can exhibit

vastly dissimilar physical and mechanical properties including: density, hygroscopicity, solubility, dissolution rate, hardness, and compactibility. Therefore, characterization of different polymorphic forms can be vital to successful development and stability of drug products.

Both IGC SEA and DVS have been successfully used previously to characterize different polymorphs. For instance, DVS was used to show that four Neotame anhydrate polymorphs exhibited unique water sorption properties. In particular, the four polymorphs showed a clear trend in ease of converting to the monohydrate form [10]. Also, different polymorphic forms of Salicaine were readily differentiated and identified by their unique water sorption isotherms [11]. Other gravimetric vapor sorption studies on different polymorphs also elucidated clear differences in moisture sorption behavior [12,13].

Different polymorphic forms often have different free energy values, making IGC SEA surface free energy measurements an ideal technique to study polymorphs. For instance, IGC SEA was used to study two polymorphs of Xemilofiban, where polymorph A had a dispersive surface energy of 49.8 mJ/m^2 and polymorph B was 42.9 mJ/m^2 [14]. Polymorph B was known to be more thermodynamically stable form, which should have a lower free energy. Therefore, the lower surface energy value was consistent (but not necessarily determinant) with the more stable crystal form. After milling and exposing polymorph A to high humidity conditions, it did not relax to the more stable polymorph, indicating it was kinetically stable (see Table 1). Additionally, the surface energy and acid/base properties of different Salmeterol Xinafoate polymorphs were studied by IGC SEA [15,16,17]. The metastable Form II polymorph had a higher surface energy, entropy, and a more polar surface compared to the stable Form I polymorph [15].

Table 1. Dispersive surface energy values for two Xemilofiban polymorphs at 30 °C.

Sample	Dispersive Surface Energy (mJ/m2)
Polymorph B	42.9
Polymorph A	49.8
Polymorph A (milled)	50.4
Polymorph A (milled and humidified)	50.6

Hydrates and Solvates

Hydrates and solvates represent another important classification of crystalline pharmaceutical materials. Approximately one-third of organic materials are capable of forming hydrates or solvates [18]. Solvates are not technically polymorphs, because solvates are crystals with different numbers of solvent molecules, while polymorphs are different structures of the same molecules. The solvation state is dependent on both temperature and solvent vapor pressure above the solid. As with higher energy polymorphs, solvated materials can also be metastable at the appropriate conditions. The solvation state of a material may influence several material properties including physical and chemical stability. The physico-chemical stability of solvates is of particular concern, because during desolvation they may convert to an amorphous form or become chemically labile [19]. Also, different solvate forms can affect the material dissolution rate, flowability and compressibility. These factors affect the entire chain of the drug development process from preformulation to manufacturing to packaging and storage.

DVS is widely used to investigate solvate formation, particularly hydrates. The conversion from the unsolvated state to the solvated state is a first order phase transformation. Whether formed from the liquid or vapor phase, both solvation-desolvation processes are thermodynamically equivalent. If both processes are performed under equilibrium conditions, then the solvation-desolvation transition should occur at the same solvent activities in both liquid and

vapor phases [20]. Therefore, solvate formation measured by vapor sorption techniques indicates where similar transitions would occur in the liquid-phase. However, the kinetics of these transitions may be vastly different in the vapor phase, compared to the liquid phase.

Stoichiometric hydrate and solvate formation by DVS are explained in detail in References 21 and 22, respectively. If the molecular weight of the anhydrous material is known, it is possible to determine the stoichiometry of the solvate. To illustrate, Figure 2 displays the acetone sorption isotherms of anhydrous carbamazepine. Below 85% P/Po the sample does not adsorb any appreciable acetone vapor. Above this point, the sample absorbs 23.7% of its dry weight in acetone vapor. This is due to formation of a 1:1 solvate with acetone. During desorption, the solvated acetone molecule is not removed until the sample is exposed to acetone vapor concentration below 10% P/Po. The 'square' hysteresis is typical for stoichiometric solvates formed during a DVS experiment. More details on the acetone vapor induced solvation of carbamazepine can be found in paper [23].

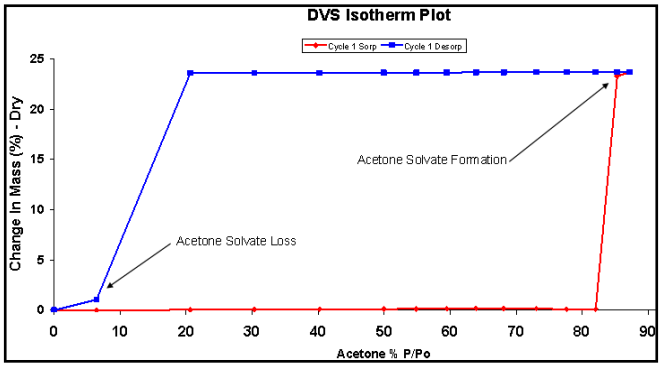

Figure 2. Acetone vapor sorption (red) and desorption (blue) isotherms for carbamazepine at 25 °C.

Non-stoichiometric hydrates can exist in channel, cage and layer configurations. DVS has also been used previously to study channel hydrates [24]. In this study, both stoichiometric trihydrate and channel hydrate forms were clearly identified by their respective water sorption isotherms. Gravimetric vapor sorption methods have also been used to study the affect of excipients on hydrate-anhydrate phase transformations [25]. Gravimetric vapor sorption methods have the added benefit of being able to investigate the kinetics of dehydration [26, 27] and desolvation [23].

A final area of characterization in the formation of hydrates/solvates of pharmaceutical materials is the combined use of DVS with *in-situ* vibrational spectroscopy. As moisture is absorbed by a sample, the intermolecular structure and forces within it adapt to accommodate water molecules. This leads to changes in the sample's molecular vibrational characteristics, which can be monitored by changes in the Raman spectrum [28] or Near-IR spectrum [29]. To illustrate, Figure 3 shows the Raman spectra for Nedocromil sodium at 13 and 15% RH [28]. DVS water sorption data in this region indicates the absorption of two moles of water. The Raman spectra confirm the transition from the monohydrate to the tri-hydrate state. As the compound changes hydration state, substantial modifications in pharmaceutically important properties can occur, such as solubility and bio-availability of the drug. Further, the hyphenization of Near-IR spectroscopy with DVS was able to correlate changes to the –OH peak to changes in the hydrated state of crystalline raffinose [29]. The sample started as the penta-hydrate form but during drying the penta-, tetra-, tri-, and di-hydrate forms could be identified by the Near-IR spectra.

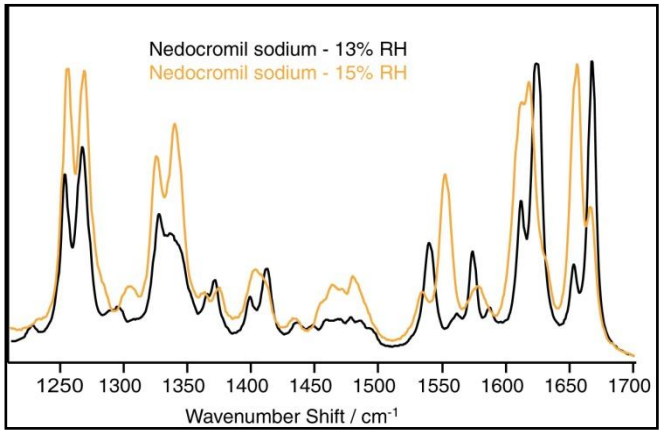

Figure 3. Spectra of nedocromil sodium at 13% and 15% RH.

Anisotropic Nature of Crystals

Crystalline materials can be energetically anisotropic, meaning the surface chemistry is not homogeneous or different crystal planes can exhibit different chemistry. Wetting experiments on macroscopic crystals have clearly shown differences in surface energy between different crystal planes of active pharmaceutical ingredients [30,31]. The habits of the macroscopic paracetamol single crystals grown from both methanol and acetone correspond to those reported in the literature, with major facets of (201), (001), (011), and (110). Further, IGC SEA experiments on milled paracetemol indicated that milling preferentially exposed the (010) facet of paracetamol form I crystals, whereas for unmilled samples the (201) facet dominated [32]. This is illustrated in Table 2 (data obtained from Reference 32) where there is little difference in dispersive surface energy values for the unmilled crystals, but the smaller, milled crystals have a significantly higher dispersive surface energy. For instance, at particle size fractions between 75 and 125 µm, the milled samples have a dispersive surface energy of 39.9 mJ/m^2, while the unmilled value is only 31.26 mJ/m^2. This is due to milling exposing the (010) crystal facet [30,32]. Changes in wettability upon milling can ultimately affect granulation behavior. Therefore, even for crystalline materials, it is important to treat them as energetically heterogeneous materials, and their surface energy may not be adequately described by a single value. Finite concentration IGC SEA experiments allow for the determination of surface energy distributions which more accurately describe the anisotropic surface energy for real materials. Surface energy distributions will be reviewed in a later section.

Table 2. Dispersive surface energy values for unmilled and milled paracetemol crystals grown from acetone solution at different particle size fractions.

Paracetemol Crystals (from Acetone Solution)	Dispersive Surface Energy (mJ/m^2) at Different Particle Sizes (µm)						
	32-75	75-125	125-150	150-250	250-425	425-600	725
Unmilled	-	31.26	30.67	30.67	31.20	32.32	32.91
Milled	41.0	39.3	39.6	37.8	37.6	34.0	-

Crystalline Defects

Crystalline materials are rarely perfect. In fact, even single crystals will have a structure that consists of boundaries, vacancies, kinks, and other defect sites. Additionally, processing steps, such as milling, spray-drying, freeze-drying, granulation, and compaction can induce varying degrees of disorder to crystalline materials. Crystalline defects may behave differently from the amorphous form as observed in one study on Griseofulvin [33]. Due to the high sensitivity to subtle surface changes, IGC SEA is an ideal technique for studying such process-induced disorder. For instance, IGC SEA has recently been employed to study the changes in surface properties due to milling [32,34,35]. In one study, the surface of Cefditoren Pivoxil became increasingly basic as milling conditions became more aggressive. The authors attributed this change in surface chemistry due to exposure of carbonyl groups which were initially below the surface on the crystalline starting material [34]. If disorder increases by processing or intentional creation, then pharmaceutical materials can become (partially) amorphous.

Amorphous or Partially Amorphous Materials

As previously stated, whether induced intentionally or unintentionally, the presence of the amorphous phase can yield unique challenges in the formulation, processing, and storage of these materials. The subsequent sections will highlight how IGC SEA and DVS have been employed to identify and characterize the amorphous phase.

Identification of the Amorphous Phase

IGC SEA has been used in several papers to identify clear differences between the amorphous and crystalline phases [34,35,36]. Not only is IGC SEA sensitive to the creation of amorphous materials, but it can also identify differences in surface energy for amorphous materials created through different routes. Table 3 displays the dispersive surface energy for crystalline α-lactose monohydrate and (partially) amorphous lactose created through different processes. Crystalline α-lactose monohydrate has a much lower dispersive surface energy value (37.6 mJ/m^2) compared to the amorphous lactose samples. However, the dispersive surface energy values for the amorphous lactose samples ranged from 43.2 mJ/m^2 for the spray-dried lactose sample to 50.7 mJ/m^2 for the super-critical freeze-dried lactose sample. The values for the spray-dried, freeze-dried and super-critical freeze-dried materials in Table 3 were measured on samples of similar amorphous contents, so the differences cannot be explained by varying degrees of crystallinity, but rather due to differences in active surface chemistry.

Table 3. Dispersive surface energy values for amorphous lactose through different processing routes.

Sample	Dispersive Surface Energy (mJ/m^2)
α-lactose monohydrate	37.6
Spray-dried lactose	43.2
Freeze-dried lactose	48.1
Super-critical freeze-dried lactose	50.7

DVS has also been used successfully to indentify differences between the crystalline and amorphous phases. To illustrate, the kinetics of hydration for anhydrous theophylline studied by DVS was found to be vastly different for the crystalline and amorphous phases [37]. Using DVS with *in-situ* Raman spectroscopy, it has been shown that for Disodium cromoglycate both the crystallinity and the water content decrease gradually as the relative humidity of the environment is decreased during dehydration, suggesting that the transition between the crystalline form and the amorphous form cannot be precisely defined [28]. Also, DVS in combination with near-IR spectroscopy has been used to identify differences between crystalline and amorphous raffinose [29].

Quantifying Amorphous Contents below 5%

There are numerous techniques available to quantify moderate to high levels of amorphous material in powders. Some of these techniques include: differential scanning calorimetry (DSC), density, powder x-ray diffraction, thermal stimulated current spectroscopy, solution calorimetry, FT-Raman, Near IR, and modulated DSC. However, there are few techniques available to quantify amorphous contents below 1%. These techniques include: solid state NMR, microflow calorimetry, and parallel beam powder X-ray diffraction. One of the most sensitive and reproducible techniques is gravimetric vapor sorption.

There are several methods in the literature using gravimetric vapor sorption techniques to quantify amorphous contents [38,39,40,41,42]. Most of these methods are based on the amorphous phase sorbing more vapor than the crystalline phase. Amorphous materials typically have a higher surface area and vapor affinity than their crystalline counterparts. For vapor sorption methods a calibration of known amorphous contents is typically necessary. Then, the equilibrium vapor uptake at a particular vapor concentration is plotted versus the known amorphous content. The result is a calibration curve to which unknown amorphous contents can be compared. Due to the above mentioned changes in crystalline state induced by water (solvation, polymorph conversion, etc.), use of a non-polar organic vapor is recommended for hydrophobic materials. To illustrate, Figure 4 shows the octane vapor sorption isotherms (a.) and calibration curve (b.) for lactose samples with varying amorphous contents. The error margins in Figure 4b were based on the 1st standard deviation for repeat measurements (n=3).

Amorphous standards were created by making physical mixtures of 100% amorphous and 100% crystalline lactose. The resulting calibration curve and correlation coefficient (R^2=0.9994) suggests that amorphous contents below 0.5% were achievable with an accuracy of ± 0.3%. Other vapor sorption approaches have also been able to quantify amorphous contents below 1% with similar accuracies [38,39,40,41].

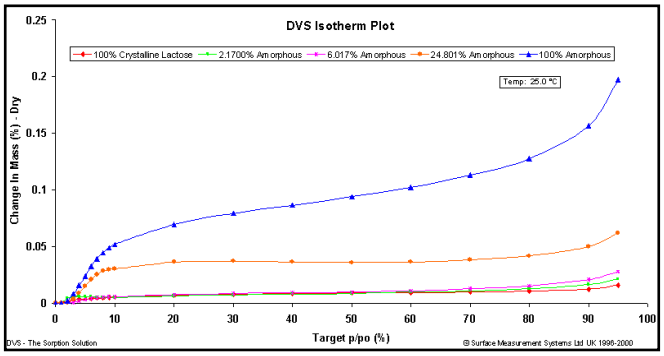

(a)

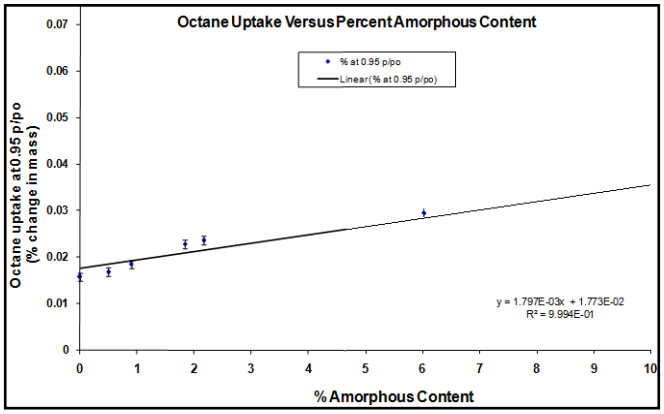

(b)

Figure 4. Octane vapor sorption isotherms (a.) and resulting calibration curve (b.) for lactose samples with various amorphous fractions.

Glassy to Rubbery Transition

As an amorphous material passes through the glass transition it often transforms from a glassy, hard, brittle material to a less viscous, 'rubber' state [43]. Additionally, there is a shift in the molecular mobility of amorphous compounds at the glass transition [44]. Above the glass transition, the molecular mobility increases as evidenced by a decrease in viscosity and increasing flow properties. Temperature often forces the transformation at a characteristic temperature or temperature range (i.e. T_g). IGC SEA can be used to determine glass transition temperatures for pharmaceutical materials [45,46,47,48]. This is typically observed by a dramatic shift in retention volume as the sample passes through the glass transition. Below the T_g the retention volume will be dominated by surface adsorption, while above the T_g, bulk absorption affects dominate, leading to higher retention volumes. IGC SEA has the unique advantage of being able to quantify glass transition as a function of background relative humidity. By studying glass transitions over a range of humidity conditions, the plasticizing affect of water can be investigated. Table 4 shows the glass transition temperature of α-D-maltose over a range of relative humidity conditions. As expected, the glass transition temperature decreases dramatically as the humidity increases.

Table 4. Glass transition temperature for α-D-maltose at different relative humidity conditions as measured by IGC SEA.

Relative Humidity (%)	Glass Transition Temperature
0	88.5 °C (361.6 K)
5	75.5 °C (348.6 K)
10	65.7 °C (338.8 K)
15	59.4 °C (332.5 K)

As illustrated above, water is a common plasticizer, thus the water content in amorphous foods, polymers, and pharmaceutical materials can have a significant lowering effect on the glass transition temperature. DVS can be used to study moisture-induced glass transitions. If the humidity surrounding an amorphous material is linearly ramped from 0% relative humidity (RH) to a humidity above the water vapor induced glass transition, then a shift in vapor sorption characteristics will be evident. Below the glass transition, water sorption will typically be limited to surface adsorption. As the material passes through the glass transition, molecular mobility increases, allowing bulk water absorption.

Therefore, the shift in sorption characteristics can be used as a measure of the glass transition.

Above the glass transition, some amorphous materials will relax to their more stable, crystalline state. As mentioned above, the amorphous material will typically have a greater water vapor sorption capacity than the crystalline material, due to increased void space, free energy, and/or surface area. When the material undergoes an amorphous to crystalline transition, the water sorption capacity typically decreases drastically. This results in an overall mass loss as excess water is desorbed during crystallization. This transition mass loss can be used to isolate the particular humidity at which glass transition and crystallization occurs.

To illustrate, Figure 5 displays a 6% RH/hour humidity ramping experiment for an amorphous lactose sample. Below the glass transition, water sorption will be dominated by surface adsorption. Above the glass transition, water sorption is dominated by bulk absorption. The transition point between these two regimes is taken as the vapor-induced glass transition. In Figure 5, this occurs around 40% RH. If the values are extrapolated to a 0% RH/hour ramping rate a value of 30% RH is obtained. This technique has been used previously on different materials with results similar to those found by DSC and IGC SEA [49]. As the humidity is increased and water vapor further plasticizes the sample, some low molecular weight materials may relax to the crystalline state. This is observed in Figure 5 by the sharp mass loss above 60% RH. At an extrapolated ramping rate of 0% RH/hour a value of 58% RH is obtained for the crystallization humidity. Again, this correlates well to other vapor studies on amorphous lactose [49]. The physical changes inferred from the gravimetric data can be further supported by *in-situ* microscopic images collected during the experiment. Figure 6 shows 100x images of amorphous lactose taken at 0% (A), 50% (B), 60% (C), and 90% RH (D). By 50% RH the sample is clearly changed to the rubbery form due to the humidity-induced glass transition. By 60% RH, the sample begins to crystallize, where at 90% RH crystallization of amorphous lactose is evident by an increase in the opacity of the image. When combined with the change in mass results in Figure 5, the images shown in Figure 6 clearly identify different humidity-induced phase changes.

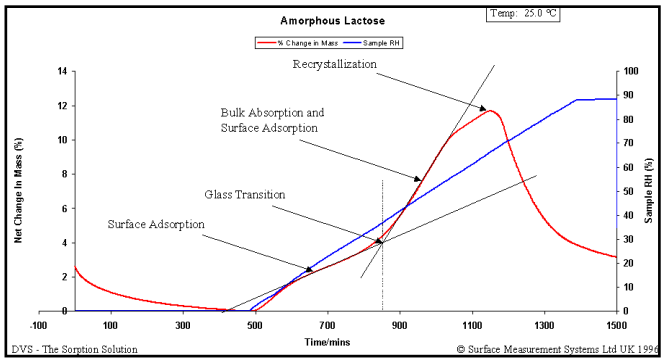

Figure 5. Humidity ramping experiment for amorphous lactose showing humidity induced glass transition and crystallization.

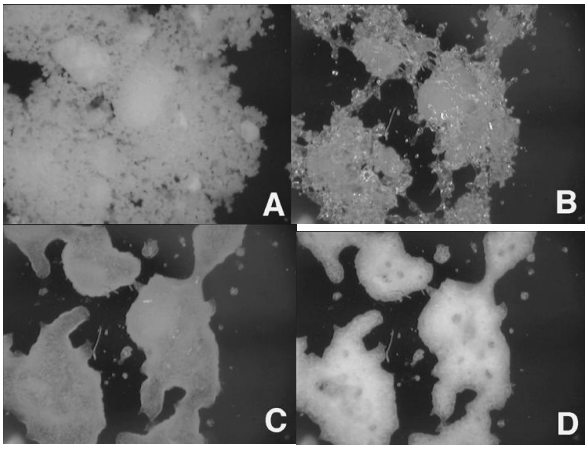

Figure 6. In-situ images collected on amorphous lactose at 0% (A), 50% (B), 60% (C), and 90% RH (D).

Vapor-Induced Crystallization

As shown above, when an amorphous material undergoes a vapor-induced crystallization, there is often a sharp mass loss due to the lower surface area, surface energy, and/or void spaces in the crystalline phase (i.e. density). This mass loss can be used to monitor the crystallization reaction. Figure 7 shows the moisture-induced crystallization behavior for amorphous lactose exposed to 55% RH at 25 °C. The distinct mass

loss feature observed around 900 minutes is due to crystallization of the amorphous lactose. Crystallization is complete by ~1200 minutes in Figure 7.

If experiments similar to that shown in Figure 7 are performed at different temperature or solvent conditions, then the crystallization mechanism can be elucidated. Then, crystallization behavior can be predicted over a wider range of vapor concentration and temperature conditions. Figure 8 shows the crystallization behavior for an amorphous lactose sample at 51% RH and different temperatures. The scale has been normalized such that time equal to zero is set to the point at which crystallization begins. Further, the y-axis is normalized to fraction crystallized (1=completely amorphous and 0=completely crystalline). When processed with a mechanistic modeling package, the data in Figure 8 resulted in a mechanism with two competing, two-step reactions. Complete details on the crystallization mechanism can be found in Reference [50]. Once the mechanism is determined, it is possible to predict the crystallization behavior of the amorphous phase over a wide range of storage, processing, and packaging conditions. This approach can also be used to study other solid-state transitions like dehydration, hydration, or solvation [51,52,53].

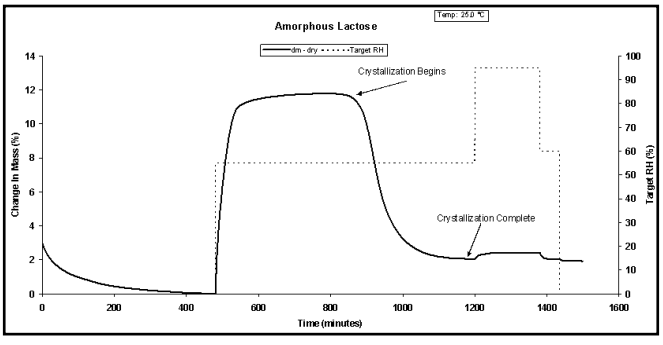

Figure 7. Amorphous lactose crystallization at 55% RH and 25 °C.

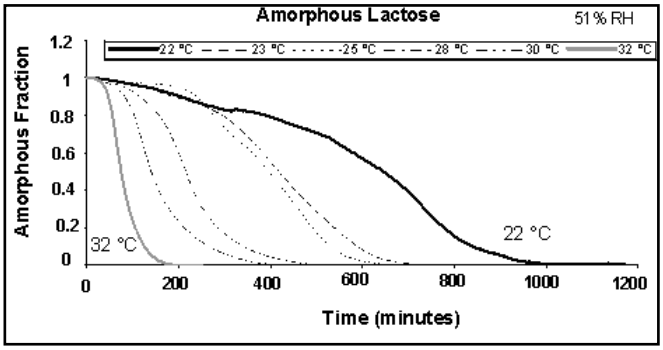

Figure 8. Humidity-induced lactose crystallization at 51% RH between 22 and 32 °C.

Energetic Relaxation

Drug substances that are intended for delivery via the lung are often micronized to reduce the particle size to the respirable range of below 6 µm. These high-energy processes often change surface morphology, increase defect sites, or decrease crystallinity. It is important to understand how these high-energy sites relax over time at different storage/exposure conditions. A recent study by SMS monitors the surface chemistry of a milled budesonide sample after exposure to 52% relative humidity and 25 °C as a function of exposure time using IGC SEA. After exposure to these conditions, the dispersive surface energy was relatively constant until after 30 days where it drops moderately (Figure 9a). In contrast, the surface basicity decreases (or surface acidity increases) precipitously as 52% RH exposure time increases, as illustrated by the Ka/Kb ratio in Figure 9b. This suggests a reorientation of polar surface groups and might therefore affect the adhesion/cohesion force balance of budesonide in a typical binary DPI formulation.

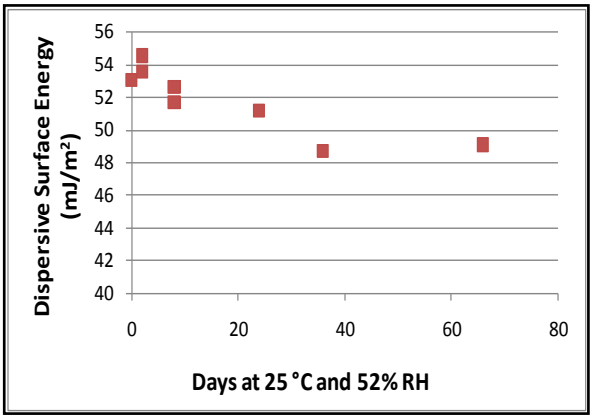

(a)

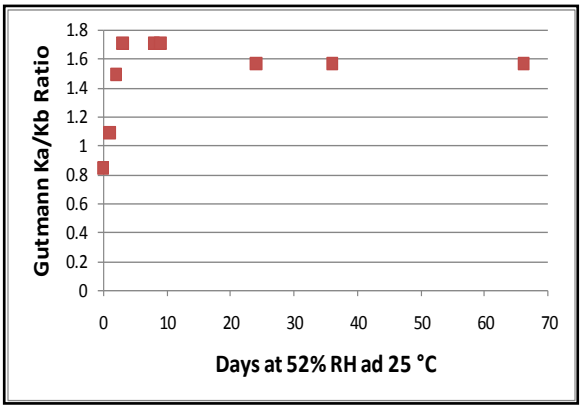

(b)

Figure 9. Dispersive surface energy (a.) and Guttmann Ka/Kb ratios (b.) for a milled budesonide sample measured at different storage exposures of 52% RH and 25 °C.

Surface Energy Heterogeneity

The anisotropic nature of crystals, different functional groups, impurities, defect sites, and varying levels of amorphous content make most materials energetically heterogeneous. For these reasons, it may be beneficial to measure a distribution or range of surface energies for a particular material. Traditional IGC SEA experiments are typically performed at infinite dilution where only interactions with the most energetic sites are measured. To include lower energy sites, higher vapor concentrations (finite concentration) are injected. In the past, researchers have used IGC SEA to measure adsorption potential or adsorption energy distributions in order to determine the energetic heterogeneity of solids [23,54,55,56]. However, these values are probe molecule dependent and not an independent property of the solid. Recent work has developed new methods for determining surface energy distributions for powders using IGC SEA [57,58]. For the first time, these exciting new methods allow the direct measurement of dispersive surface energy profiles as a function of surface coverage. Measuring energetic heterogeneity profiles could provide valuable information in the characterization of complex surfaces. To illustrate, Figure 10 shows the dispersive surface energy as a function of surface coverage (value of 0 is at zero coverage or infinite dilution, value of 1 is for complete surface coverage) for three different lactose samples [57]. For the milled material there is a shift in the energy distribution of dispersive surface energy to higher values, compared to the other two samples. In combination with DVS amorphous content results (see Quantifying Amorphous Content section above) the IGC SEA heterogeneity data suggests that the milled sample has a significant amount of amorphous material. The amorphous content of the untreated and recrystallized sample is extremely small. Although untreated and recrystallized lactose showed a similar dispersive surface energy at infinite dilution the energy distributions for the two samples are quite different. The recrystallized sample has a more uniform distribution, suggesting a more energetically homogenous surface.

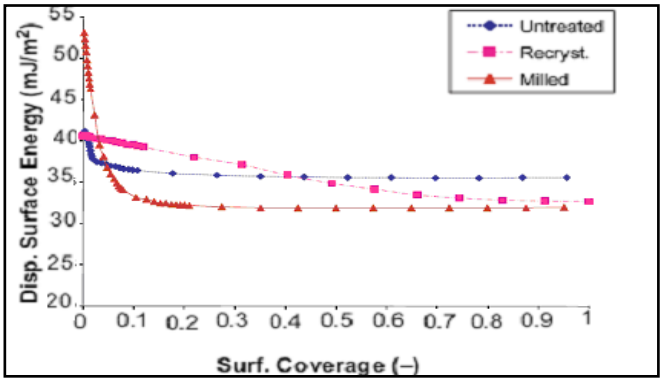

Figure 10. Dispersive surface energy profile for untreated (blue), crystalline (pink), and milled (red) lactose sample.

Conclusion

Pharmaceutical materials range in complexity from well-ordered materials with a defined crystal lattice to completely amorphous materials with no long-range order. The level of disorder or thermodynamic instability of the material can affect every step of pharmaceutical development from formulation and processing to storage and stability. These challenges make characterizing solid materials paramount in successful pharmaceutical product development and quality by design. Vapor sorption techniques like DVS and IGC SEA have proven to be valuable techniques for the determination of a wide range of physico-chemical properties. In this review, numerous examples illustrate how DVS and IGC SEA can be used to characterize crystalline and disordered materials including polymorphs, hydrates, defect sites, and amorphous materials. The unique information accessed through DVS and IGC SEA experiments can add important insight for characterizing and developing solid pharmaceutical materials.

Acknowledgement:

Many thanks to Dr. Jerry Heng from the London Imperial College, Frank Thielmann from Novartis and Ron Gray from Surface Measurement Systems for their valued discussions and contributions.

References

[1] Hancock, B.C. and Zografi, G., Journal of Pharmaceutical Science, **86** (1997) 1-12.
[2] Kontny, M.J. and Zografi, G., "Sorption of Water by Solids" in *Physical Characterization of Pharmaceutical Solids*. Brittain, H.G. editor, Marcel Dekker, New York, p387-418.
[3] Hancock, B.C. and Shamblin, S., Pharmaceutical Science and Technology Today, **1** (1998) 345-351.
[4] Condor J, Young C. *Physicochemical measurement by gas chromatography*. John Wiley and Sons, Chichester, UK (1979).
[5] Thielmann, F., Journal of Chromatography A, **1037** (2004) 115-123.
[6] Buckton, G. and Gill, H. Advanced Drug Delivery Reviews, **59** (2007) 1474-1479.
[7] Domingue, J., Burnett, D.J., and Thielmann, F., American Laboratory, **7** (2003) 32.
[8] Brittain, H.G. editor, *Polymorphism in Pharmaceutical Solids*, John Wiley and Sons, New York (1998).
[9] Carstensen, J.T., in *Solid Pharmaceuticals: Mechanical Properties and Rate Phenomena*, Academic Press, New York (1980).
[10] Dong, Z., Padden, B.E., Salsbury, J.S., Munson, E.J., Schroeder, S.A., Prakash, I., and Grant, D.J.W., Pharmaceutical Research, **19** (2002) 330-336.
[11] Schmidt, A.C., Schwarz, I., and Mereiter, K., Journal of Pharmaceutical Sciences, **95** (2006) 1097-1112.
[12] Carvajal, M.T. and Staniforth, J.N., International Journal of Pharmaceutics, **307** (2006) 216-224.
[13] Guerrieri, P., Salameh, A.K., and Taylor, L.S., Pharmaceutical Research, **24** (2006) 147-156.
[14] SMS Application Note 207.
[15] Tong, H.H.Y., Shekunov, B.Y., York, P., and Chow, A.H.L., Pharmaceutical Research, **19** (2002) 640-648.
[16] Tong, H.H.Y., Shekunov, B.Y., York, P., and Chow, A.H.L., Pharmaceutical Research, **18** (2001) 852-858.
[17] Tong, H.H.Y., Shekunov, B.Y., York, P., and Chow, A.H.L., Journal of Pharmaceutical Sciences, **94** (2005) 695-700.
[18] Henck, J.O., Griesser, U.J. and Burger, A., Pharm. Ind., **59** (1997) 165-169.
[19] Khawam, A. and Flanagan, D.J., J. Pharm. Sci., **95** (2006) 472-498.
[20] Beckmann, W., and Winter, G., Industrial Crystallization (1999) 1-10.
[21] SMS Application Note 36.
[22] SMS Application Note 41.
[23] Burnett, D.J., Thielmann, F., and Sokoloski, T., Journal of Thermal Analysis, **89** (2007) 693-698.
[24] Vogt, F.G., Brum, J., Katrincic, L.M., Flach, A., Socha, J.M., Goodman, R.M., and Haltiwanger, R.C., Crystal Growth and Design, **6** (2006) 2333-2354.
[25] Salameh, A.K. and Taylor, L.S., Journal of Pharmaceutical Sciences, **95** (2006) 446-461.
[26] Manek. R.V. and Kolling, W.M. AAPS PharmSciTech, **5** (2004) Article 14, 1-8.
[27] Surana, R., Pyne, A., and Suryanarayanan, R., AAPS PharmSciTech, **4** (2003) Article 4, 1-10.
[28] SMS Application Note 507.
[29] Hogan, S.E. and Buckton, G., International Journal of Pharmaceutics, **227** (2001) 57-69.
[30] Heng, J.Y.Y., Bismark, A., Lee, A.F., Wilson, K., and Williams, D.R., Langmuir, **22** (2006) 2760-2769.
[31] Heng, J.Y.Y., Bismark, A., and Williams, D.R., AAPS PharmSciTech, **7** (2006) Article 84, E1-E9.
[32] Heng, J.Y.Y., Thielmann, F., and Williams, D.R., Pharmaceutical Research, **23** (2006) 1918-1927.

[33] Feng, T., Pinal, R., and Carvajal, M.T., Journal of Pharmaceutical Sciences, **97** (2008) 3207-3221.
[34] Ohta, M. and Buckton, G., International Journal of Pharmaceutics, **269** (2004) 81-88.
[35] Newell, H.E., Buckton, G., Butler, D.A., Thielmann, F., and Williams, D.R., Pharmaceutical Research, **18** (2001) 662-666.
[36] Feeley, J.C., York, P., Sumby, B.S., and Dicks, H., International Journal of Pharmaceutics, **172** (1998) 89-96.
[37] Debnath, S. and Suryanarayanan, R., AAPS PharmSciTech, **5** (2004) Article 8, 1-11.
[38] Hancock, B.C. and Zografi, G., Journal of Pharmaceutical Science, **86** (1997) 1-12.
[39] Saleki-Gerhard, A., Ahlneck, C., and Zografi, G., International Journal of Pharmaceutics, **101** (1994) 237.
[40] Buckton, G., and Darcy, P. Proc. 1st World Meeting APGI/APV, Budapest, 9/11 May 1995.
[41] Mackin, L., Zanon, R., Park, J.M., Foster, K., Opalenik, H, and Demonte, M., International Journal of Pharmaceutics, **231** (2002) 227.
[42] Young, P.M., Chiou, H., Tee, T., Traini, D., Chan, H.-K., Thielmann, F., and Burnett, D., Drug Development and Industrial Pharmacy, **33** (2007) 91-97.
[43] Sperling, L.H., *Introduction to Physical Polymer Science.* John Wiley & Sons, New York (1986).
[44] Roos, Y.H., *Phase Transitions in Foods.* Academic Press, New York (1995).
[45] Thielmann, F., Attwool, P., and Tojo, M., Nippon Yakugakkai Nenkai Koen Yoshishu, **123** (2003) 53.
[46] Buckton, G., Ambarkhane, A., and Pincott, K., Pharmaceutical Research, **21** (2004) 1554-1557.
[47] Ambarkhane, A.V., Pincott, K., and Buckton, G., International Journal of Pharmaceutics, **294** (2005) 129-135.
[48] Surana, R., Randall, L., Pyne, A., Vemuri, N.M., and Suryanarayanan, R., Pharmaceutical Research, **20** (2003) 1647-1654.
[49] Burnett, D.J., Thielmann, F., and Booth, J., International Journal of Pharmaceutics, **287** (2004) 123-133.
[50] Burnett, D.J., Thielmann, F., Sokoloski, T., and Brum, J., International Journal of Pharmaceutics, **313** (2006) 23-28.
[51] Khawam, A. and Flanagan, D.R., Journal of Pharmaceutical Sciences, **95** (2006) 472-498.
[52] Sheth, A.R., Zhou, D., Muller, F.X., and Grant, D.J.W., Journal of Pharmaceutical Sciences, **93** (2004) 3013-3026.
[53] Burnett, D.J., Thielmann, F., and Sokoloski., T.D., Journal of Thermal Analysis, **89** (2007) 693-698.
[54] Charmas, B. and Leboda, R., Journal of Chromatography A, **886** (2000) 133-152.
[55] Balard, H., Macromolecules, **11** (1978) 228.
[56] Thielmann, F. and Pearse, D., Journal of Chromatography A, **969** (2002) 323-327.
[57] Thielmann, F., Burnett, D.J., and Heng, J.Y.Y., Drug Development and Industrial Pharmacy, **33** (2007) 1240-1253.
[58] Ylä-Mäihänemi, P.P., Heng, J.Y.Y., Thielmann, F., and Williams, D.R., Langmuir (2008) *in press*.

Head Office:
Surface Measurement Systems, Ltd
5 Wharfside, Rosemont Road
London HA0 4PE, UK
Tel: +44 (0)20 8795 9400
Fax: +44 (0)20 8795 9401
Email: science@surfacemeasurementsystems.com

United States Office:
Surface Measurement Systems, Ltd, NA
2125 28th Street SW, Suite I
Allentown PA, 18103, USA
Tel: +1 610 798 8299
Fax: +1 610 798 0334



